Extended Bennia–Riad Criterion for Iterative Frequency-Domain Deconvolution

Tom Dhaene, Luc Martens, *Member, IEEE* and Daniël De Zutter, *Member, IEEE*

***Abstract*—In this paper, we present a new, fast, robust and accurate iterative frequency-domain deconvolution technique. The deconvolution problem is mathematically classified as an ill-posed problem. We propose a new generalized deconvolution filter, and we use the so-called *extended "Bennia-Riad" criterion* to determine the optimal filter parameters.**

I. Generalized Deconvolution Filter

CONSIDER a linear time-invariant system with an impulse reponse $h(t)$ (Fig. 1). $x(t)$ and $y(t)$ are the input and output response, respectively. Let $x_m(t)$ and $y_m(t)$ be the measured input and output response. Averaging may be used to increase the signal/noise ratio of the measurements. $H(f), X(f), Y(f), X_m(f)$, and $Y_m(f)$ are the corresponding frequency-domain representations. Due to the inevitable measurement errors, the transfer function $H(f)$ cannot be found exactly starting from $X_m(f)$ and $Y_m(f)$. We define the optimal transfer function $H_{\text{opt}}(f)$ as

$$H_{\text{opt}}(f) = Y_m(f)F(f)/X_m(f) = H_m(f)F(f) \quad (1)$$

where $F(f)$ is a (real positive) regularization filter introduced to reduce the deconvolution noise. This filter must compensate all kinds of measurement errors. The choice of this filter is subjective.

We formulate a new general cost function K_{tot} which maximizes the smoothness of the deconvolved results, and minimizes the deconvolution errors and the unwanted peaks (caused by a division by nearly zero) over the frequency range $[0 - f_{\text{MAX}}]$ which is useful for the envisaged application:

$$K_{\text{tot}} = K_{\text{error}} + \gamma K_{\text{smooth}} + \lambda K_{\text{peak}} \quad (2)$$

where

$$K_{\text{error}} = \int_0^{f_{\text{MAX}}} |Y_m(f) - H_{\text{opt}}(f)X_m(f)|^2 \, df \quad (3)$$

$$K_{\text{smooth}} = \int_0^{f_{\text{MAX}}} |(j\omega)^p H_{\text{opt}}(f)|^2 \, df \quad (4)$$

$$K_{\text{peak}} = \int_0^{f_{\text{MAX}}} |H_{\text{opt}}(f)|^2 \, df. \quad (5)$$

p is a positive even number. γ and λ are real positive weighing factors.

Manuscript received May 18, 1993; revised October 8, 1993. This work was supported in part by the IWONL.

The authors are with the Department of Information Technology, University of Ghent, 9000 Ghent, Belgium.

IEEE Log Number 9215990.

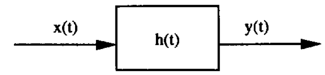

Fig. 1. Linear time-invariant system.

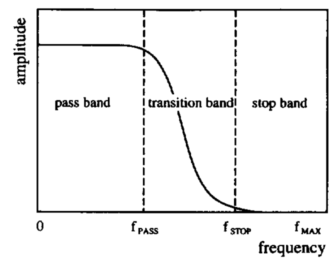

Fig. 2. Low-pass filter partitioned in three frequency regions.

The new generalized deconvolution filter $F(f)$ is found by minimizing the cost function K_{tot} (2) with respect to $F(f)$:

$$F(f, \gamma, \lambda) = \frac{|X_m(f)|^2}{|X_m(f)|^2 + \gamma\omega^{2p} + \lambda}. \quad (6)$$

The roll-off of this filter is mainly determined by the parameter p. Our new frequency-domain deconvolution filter (6) combines the advantages of the "Guillaume–Nahman filter" ($\lambda = 0$) [1] and the "optimal compensation filter" ($\gamma = 0$) [2]. The parameter γ (smoothing factor) ensures an efficient reduction of the high-frequency noise components (low-pass filter), while the parameter λ (peak reduction factor) ensures a selective reduction of the deconvolution noise (adaptive filter).

II. Extended "Bennia–Riad" Criterion

The optimal filter parameters γ and λ are calculated in the frequency domain. No time-consuming inverse Fourier transformations must be calculated as is the case in [1] (Guillaume–Nahman filter) and [2] (optimal compensation filter). We look for a compromise between noise reduction and signal integrity. The noise reduction and the filter errors are controlled in different frequency ranges. This can be seen as an extended "Bennia–Riad criterion" [3] for two filter parameters. We partition the complete frequency range $[0 - f_{\text{MAX}}]$ of the transfer function in several regions $i \, (i = 1, 2, \cdots)$ based on the information content of each interval.

For example, in the case of an ideal *low-pass filter* (Fig. 2) we have a pass band, a transition band, and a stop band [3]. The pass band $[0 - f_{\text{PASS}}]$ contains most of the relevant

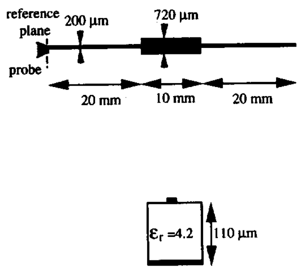

Fig. 3. Double step-in-width microstrip line.

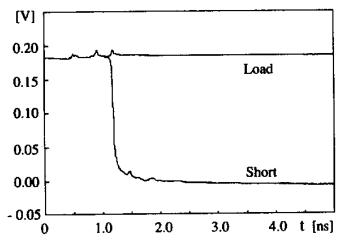

(a)

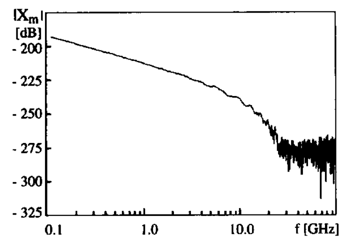

(b)

Fig. 4. (a) TDR-pictures of the 50 Ω and 0 Ω reference standards. (b) $|V_{\text{short}}(f) - V_{\text{load}}(f)|$.

frequency-domain information (large values of $|X(f)|$). The noise level in the pass band is very low. The transition band $[f_{\text{PASS}} - f_{\text{STOP}}]$ still contains a certain amount of signal information, but the noise level is no longer negligible. The stop band $[f_{\text{STOP}} - f_{\text{MAX}}]$ mainly contains noise, while the useful information content is negligible (small values of $|X(f)|$). In the case of a *high-pass filter* we also have a pass band, a transition band, and a stop band, and in the case of a *band-pass filter* we have a pass band, two transition bands, and two stop bands.

To select the optimal filter parameters, we calculate the standard deviation of the difference of the filtered and the (nearly) unfiltered transfer function as a function of the filter parameters γ and λ in all different frequency regions $i\,(i = 1, 2, \cdots)$. These so-called "noise factors" NOISE_i are defined as:

$$\text{NOISE}_i(\gamma, \lambda) = \text{RMS}_i\{|H_m(\omega)[F(f, \gamma, \lambda) - F(f, \gamma_{\min}, \lambda_{\min})]|\} \quad (7)$$

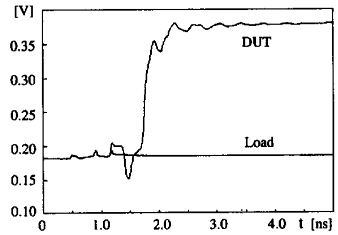

(a)

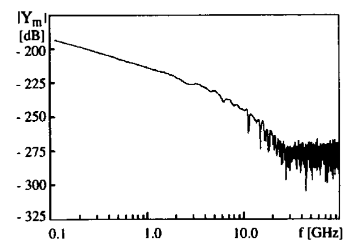

(b)

Fig. 5. (a) TDR-pictures of the 50 Ω standard and the DUT. (b) $|V_{\text{dut}}(f) - V_{\text{load}}(f)|$.

where $\gamma_{\min} \approx 0.0001\,\gamma_{\text{init}}$ and $\lambda_{\min} \approx 0.0001\,\lambda_{\text{init}}$ (see further on). The noise factors are normalized to their maximal value. If the filter parameters are too low, we have no effective noise reduction ($\text{NOISE}_i \approx 0$, for all i). On the other hand, if they are too large, the signal distortion is too high ($\text{NOISE}_i \approx 1$, for all i). We want to filter the noise as much as possible, but at the same time we want to limit the unwanted filter distortion.

For a low-pass filter, e.g., we first choose the initial filter parameters γ_{init} and λ_{init}:

$$\gamma_{\text{init}} = \frac{0.02\,|X_{\min}|^2}{(2\pi f_{\text{PASS}})^{2p}} \quad (8)$$

and

$$\lambda_{\text{init}} = 0.02\,|X_{\min}|^2 \quad (9)$$

where $|X_{\min}|$ is equal to the minimal value of $|X_m(f)|$ in the pass band $[0 - f_{\text{PASS}}]$. These initial parameters limit the maximal possible distortion in the pass band. The maximal filtering effect of the "initial deconvolution filter" is chosen to be about 4% ($1 \geq F(f, \gamma_{\text{init}}, \lambda_{\text{init}}) > 0.96, \forall f \in [0 - f_{\text{PASS}}]$). Normally, the initial filter parameters give already very good deconvolution results. Then, we vary the parameters γ and λ over some orders of magnitude, and we monitor the normalized noise factors. The noise factors of the different regions can be visualized with 3-D graphs or contour plots. The normalized noise factors must be very low in the pass band (region 1) and very high in the stop band (region 3). The "optimal" filter parameters γ_{opt} and λ_{opt} are chosen in such a way that: $\text{NOISE}_1 < 0.05, \text{NOISE}_2 \approx 0.6$ and $\text{NOISE}_3 > 0.95$. The final choice of the filter parameters remains subjective. In fact, we find a whole range of "optimal" filter parameters.

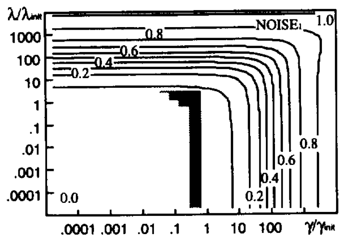

(a)

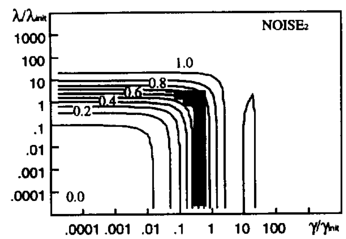

(b)

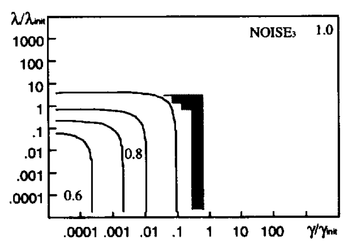

(c)

Fig. 6. Noise factors as a function of the filter parameters in (a) pass band, (b) transition band, (c) stop band.

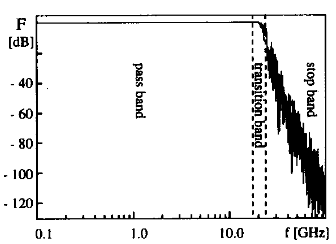

Fig. 7. Optimal deconvolution filter $F(f)$.

III. Example

In this example, we apply the new deconvolution technique to calculate the time-domain reflection coefficient $s_{11}(t)$ (reference impedance = 50 Ω) of a double step-in-width microstrip line.

The cross section and the top view of this nonuniform microstrip are depicted in Fig. 3. The right-hand side of the device under test (DUT) is open, while the left-hand side of the DUT is connected with an HP 54121T reflectometer (bandwidth ≈18.5 GHz) via high-quality 50 Ω coaxial cables and a coplanar high-frequency probe (Cascade Microtech PPH-100-150). The 50 Ω impedance and the short circuit on

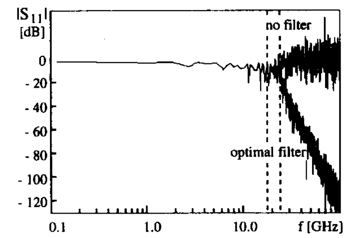

Fig. 8. Frequency-domain reflection coefficient $S_{11}(f)$.

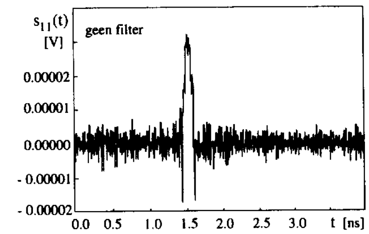

(a)

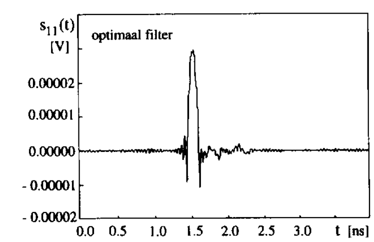

(b)

Fig. 9. Time-domain reflection coefficient $s_{11}(t)$, (a) no filter, (b) optimal filter parameters.

the Cascade Microtech "Impedance Standard Substrate" (ISS) are used to calibrate the reflectometer [4]–[7]. In Fig. 4(a), the TDR-pictures $v_{\mathrm{load}}(t)$ and $v_{\mathrm{short}}(t)$ of the reference standards are shown, and in Fig. 4(b), $|V_{\mathrm{short}}(f) - V_{\mathrm{load}}(f)|\,(= |X_m|)$ is represented. Waveform averaging is used (128 times) to improve the signal/noise ratio. The measured reflectogram of the nonuniform DUT $v_{\mathrm{dut}}(t)$ and the reference load $v_{\mathrm{load}}(t)$ are shown in Fig. 5(a). In Fig. 5(b), $|V_{\mathrm{dut}}(f) - V_{\mathrm{load}}(f)|\,(= |Y_m|)$ is depicted.

The frequency-domain reflection coefficient $S_{11}(f)$ (reference impedance = 50 Ω) is defined as [7]

$$S_{11} = -\frac{(V_{\mathrm{dut}} - V_{\mathrm{load}})}{(V_{\mathrm{short}} - V_{\mathrm{load}})} = -\frac{Y_m}{X_m}. \tag{10}$$

The parameter p of the deconvolution filter (6) is chosen to be 4.

The complete frequency range is partitioned into three frequency regions (pass band: 0–18.5 GHz, transition band: 18.5–24 GHz, stop band: 24–110 GHz). The maximal frequency f_{MAX} (= 110 GHz) is determined by the sampling rate of the reflectometer and by the FFT algorithm. The maximal frequency of the pass band f_{PASS} (= 18.5 GHz) is determined by the bandwidth of the oscilloscope. In Fig. 6,

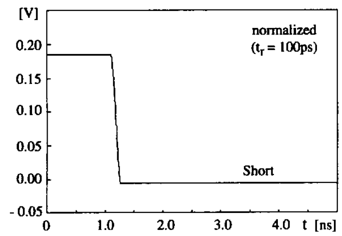

(a)

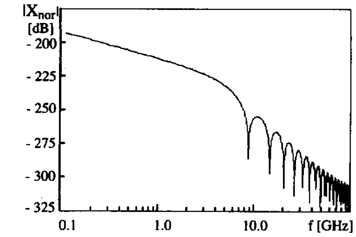

(b)

Fig. 10. (a) Normalized TDR-picture of short reference standard (rise time = 100 ps), (b) $|V_{\text{short}}^{\text{nor}}(f) - V_{\text{load}}^{\text{nor}}(f)|$.

the contour plots of the noise factors in the three frequency-domain regions are shown as a function of the filter parameters. The filter parameters are normalized to their initial guess. We have optimal filter if $\text{NOISE}_1 < 0.05, \text{NOISE}_2 \approx 0.6$, and $\text{NOISE}_3 > 0.95$. In that case we have a significant noise reduction in the stop band, a limited noise reduction in the transition band, and nearly no distortion in the pass band. The optimal filter parameters are located in the grey regions of Fig. 6. They are chosen to be: $\gamma_{\text{opt}} = 0.64\,\gamma_{\text{init}}$ and $\lambda_{\text{opt}} = 0.64\,\lambda_{\text{init}}$. The optimal filter $F(f)$ is represented in Fig. 7.

The calibrated frequency-domain reflection coefficient $S_{11}(f)$ is shown in Fig. 8 when no filter is applied and when optimal filter parameters are chosen. The corresponding time-domain impulse responses $s_{11}(t)$ are depicted in Fig. 9. The normalized time-domain reflectogram (TDR-picture) of the DUT $V_{\text{dut}}^{\text{nor}}$ is defined as [7]:

$$V_{\text{dut}}^{\text{nor}} = \left[\frac{(V_{\text{short}}^{\text{nor}} - V_{\text{load}}^{\text{nor}})}{(V_{\text{short}} - V_{\text{load}})}(V_{\text{dut}} - V_{\text{load}})\right] + V_{\text{load}}^{\text{nor}} \qquad (11)$$

where $V_{\text{short}}^{\text{nor}}$ and $V_{\text{load}}^{\text{nor}}$ are the normalized TDR-pictures of the short and the load, respectively (Fig. 10). The normalized TDR-picture of the DUT (rise time = 100 ps) is shown in Fig. 11.

IV. Conclusions

In this paper, we presented a new advanced data-processing technique for frequency-domain deconvolution. We proposed a new generalized deconvolution filter which combines the advantages of the "Guillaume–Nahman filter" and the "optimal compensation filter," and we used an extended "Bennia–Riad" criterion to determine the optimal filter parameters. This new deconvolution algorithm is much faster, more accurate, more robust and less sensitive to noise than traditional algorithms.

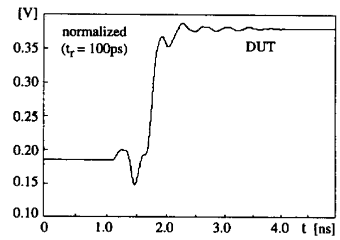

Fig. 11. Normalized TDR-picture of the DUT (rise time = 100 ps).

References

[1] N. S. Nahman and M. E. Guillaume, "Deconvolution of time domain waveforms in the presence of noise," National Bureau of Standards Tech. Note 1047, Boulder, CO, Oct. 1981.

[2] B. Parruck and S. M. Riad, "An optimization criterion for iterative deconvolution," *IEEE Trans. Instr. Meas.*, vol. IM-32, no. 1, pp. 137–140, Mar. 1983.

[3] A. Bennia and S. M. Riad, "An optimization technique for iterative frequency-domain deconvolution," *IEEE Trans. Instr. Meas.*, vol. IM-39, no. 2, pp. 358–362, Apr. 1990.

[4] Hewlett Packard, "Advanced TDR techniques," HP-Application Note 62-3, May 1990.

[5] T. Dhaene, L. Martens, P. Degraeuwe, and D. De Zutter, "Improved time-domain characterization of high-speed interconnection structures," *IEEE Topical Meet. Elec. Perform. Electron. Packaging* (IEEE-MTT & IEEE-CHMT), Tucson, AZ, Apr. 1992, pp. 142–144.

[6] T. Dhaene, L. Martens, K. De Kesel, and D. De Zutter, "Advanced calibration and normalization techniques for time domain reflection and transmission measurements," in *Proc. IEEE Inst./Meas. Technol. Conf. 1993 (IMTC/93)*, Irvine, CA, May 1993, pp. 85–87.

[7] T. Dhaene, L. Martens, and D. De Zutter, "Calibration and normalization of time domain network analyzer measurements," *IEEE Trans. Microwave Theory Tech.*, vol. 42, Apr. 1994,.

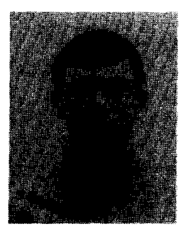

Tom Dhaene was born June 25, 1966 in Deinze, Belgium. He received the degree in electrical engineering from the University of Ghent, Belgium, in 1989. He is currently working towards the Ph.D. degree in electrical engineering at the Laboratory of Electromagnetism and Acoustics (LEA) of the same univeristy.

His research focuses on all aspects of circuit modeling, transient simulation and time domain characterization of high-frequency and high-speed interconnections.

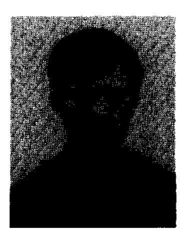

Luc Martens (M'92) was born May 14, 1963 in Ghent, Belgium. He received the degree in electrical engineering and the PH.D. degree from the University of Ghent in 1986 and 1990, respectively.

From September 1986 to December 1990, he was a Research Assistant in the Laboratory of Electromagnetism and Acoustics (LEA) at the same univeristy. During this period, his scientific work was focused on the physical aspects of hyperthermic cancer therapy. His research work dealt with electromagnetic and thermal modeling and with the development of measurement systems for that application. Since January 1991, he is still responsible at the same laboratory for the research in hyperthermia and biological effects of electromagnetic radiation but his main research activities are in the field of high frequency measurements. Since April 1993, he has been a Professor at Ghent University.

Daniël De Zutter (M'92) was born November 8, 1953 in Eeklo, Belgium. He received the degree in electrical engineering from the University of Ghent in July 1976. In October 1981 he received the Ph.D. degree there and in the spring of 1984 he completed a thesis leading to a degree equivalent to the French Aggrégation or the German Habilitation.

From September 1976 to September 1984, he was a Research and Teaching Assitant in the Department of Information Technology at the University of Ghent, where he is now a Professor and Research Director at the National Science Foundation of Belgium. Most of his earlier scientific work dealt with the electrodynamics of moving media, with emphasis on the Doppler effect and Lorentz forces. His research now focuses on all aspects of circuit and electromagnetic modeling of high-speed and high-frequency interconnections.

In 1990 Dr. De Zutter was elected as a member of the Electromagnetics Society.